Analysis of Narrow Slot Loading on a Half Guided Wavelength Folded Substrate Integrated Waveguide

Sheelu Kumari[1†], **Vibha Rani Gupta**[1], and **Shweta Srivastava**[2], Non-members

ABSTRACT

This paper presents the effects of varying the position, width, and length of a narrow slot loaded onto the central metal septum of a half guided wavelength folded substrate integrated waveguide (FSIW) segment. The study shows that the most significant effect is due to variation in slot length and that slot loading can be used both for bandwidth enhancement/slow-wave effect and filtering, depending on the length of the slot. Both phenomena are explained with the help of field diagrams for different propagating modes and an extracted circuit equivalent to the slot loaded folded substrate integrated waveguide (SFSIW) segment. The results indicate that for the designed FSIW structure, the bandwidth enhancement/slow-wave effect continues until the slot length is 3 mm ($0.18\lambda_c$), beyond which filtering is exhibited. All the developed structures can be used for space/satellite communication. This study will help in deciding the best dimensions of the slot according to the application. The measured scattering parameters of the fabricated structure are compared with the simulated results obtained from the HFSS and the circuit simulator in the ADS and considered to be in good agreement.

Keywords: Filter, Folded Substrate Integrated Waveguide, Slot Loading, Slow-Wave Structure

1. INTRODUCTION

There has been rapid growth in millimeter wave technologies for use in diverse applications, such as short-range communication, future mm-wave mobile communication for fifth-generation (5G) cellular networks, sensor imaging systems, and space communication. The substrate integrated waveguide (SIW), due to its low loss, planar nature, high integration capability, and compactness, is a good candidate for developing the operation of components and circuits in the microwave and millimeter wave region. The SIW is beneficial to both conventional high Q waveguides and low-profile planar circuits and can integrate a planar structure such as a microstrip line and non-planar structure like a waveguide, combining their advantages [1, 2]. Since the introduction of SIW technology, various SIW-based circuit components have been developed such as bends, filters, couplers, power dividers, as well as resonant cavities and antennas [3, 4]. Folded substrate integrated waveguides (FSIWs) is a compact version of the SIW [5].

Many of the microstrip based components reported in literature, utilize metallic-vias [6], defected microstrip structures (DMSs) [7], defected ground structures (DGSs) [7–11], and complementary split ring resonators (CSRRs) [12] to obtain compactness, enhanced bandwidth or stop-band characteristics. However, due to high radiation loss, microstrip based components are not suitable for high frequency applications. The SIW-based components, which are better suited for high frequency applications, also exploit the characteristics of CSSRs [13, 14], EBGs [15], DGSs [15–17], and fractals [18] to improve component performance. Slots have also been used in microstrip based [19] and SIW-based [20] structures, which is the simplest reported technique for improving the performance of components. However, to the best of the authors' knowledge, no detailed analysis of slot loading in FSIW, based on slot size has yet been reported in literature.

In this paper, a half guided wavelength FSIW segment is obtained by folding an SIW designed for a cut off frequency of 12 GHz. A slot is loaded on the central metal septum with its position, width, and length varied to study the various effects. The slot loaded folded substrate integrated waveguide (SFSIW) segment is analyzed in detail with the help of an electric field diagram and a lumped equivalent circuit. It is observed that the dimensions of the slot define the behavior of the structure as an enhanced bandwidth FSIW segment or a stop-band filter. This study focuses on the FSIW structure and will be useful for space communication [21]. Transitions

Manuscript received on August 5, 2020 ; revised on January 7, 2021 ; accepted on February 23, 2021. This paper was recommended by Associate Editor Suramate Chalermwisutkul.

[1]The authors are with the Department of Electronics & Communication Engineering, Birla Institute of Technology, Mesra, Ranchi, Jharkhand, India.

[2]The author is with the Department of Electronics & Communication Engineering, Jaypee Institute of Information Technology, Noida, India.

[†]Corresponding author: phdec10008.12@bitmesra.ac.in

Digital Object Identifier 10.37936/ecti-eec.2021192.241655

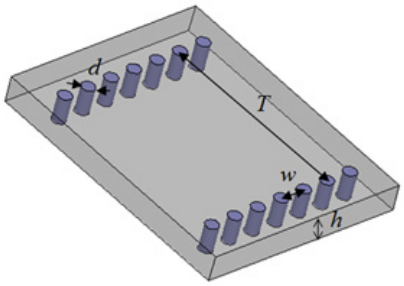

(a)

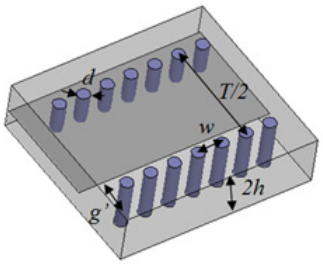

(b)

Fig. 1: *Configuration of (a) SIW and (b) FSIW.*

using the concept of simultaneous transformation in field and impedance to match the requirements of a 50 Ω microstrip line are integrated at both ends of the designed SFSIW segment.

2. DESIGN DETAILS

The SFSIW segment is obtained by loading a narrow slot onto the central metal septum of the FSIW. The required FSIW is derived from the designed SIW where $f_c = 12$ GHz.

2.1 Designing a FSIW

Initially the SIW is designed for the Ku-band with the cut off frequency $f_c = 12$ GHz and the operating frequency $f_0 = 14$ GHz using Duroid 5870 substrate with relative permittivity of $\varepsilon_r = 2.33$ and height $h = 0.787$ mm using the equations documented in [22]. The propagating mode considered is the fundamental TE_{10}.

In the next step, the proposed SIW (Fig. 1(a)) is folded into about half its width and double its height to constitute FSIW, as shown in Fig. 1(b). In Fig. 1(b), the distance between two rows of vias $T/2$ is 4.2 mm and height $2h = 1.574$ mm, while the calculated [5] and optimized distance between the center of one vias row and one edge of the central metal septum is $g = 0.3$ mm. The pitch dimensions $w = 1$ mm and the via diameter $d = 0.5$ mm are the same as for the SIW. The length of the transmission line L_g is retained at half the guided wavelength, which is 8 mm for the designed FSIW.

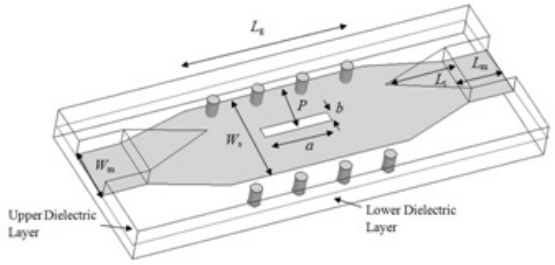

Fig. 2: *SFSIW with back-to-back transitions at two ends. (Guided wavelength of SFSIW L_g = 8 mm, width of central metal septum $W_s = 4.35$ mm, length of the perpendicular bisector of the base of the isosceles etched triangle $L_t = 3.2$ mm, length of microstrip $L_m = 2$ mm, and microstrip width W_m = 2.4 mm)*

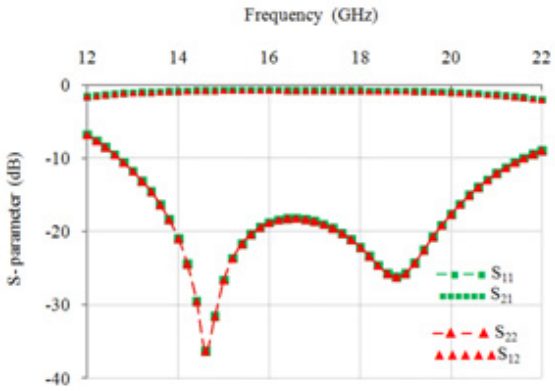

Fig. 3: *S-parameter response of FSIW segment with transitions at two ends.*

2.2 Designing Transition

Proper transitions are essential for planar circuit integration. Moreover, transitions play an important role in realizing impedance matching between the feed and circuits.

Therefore, in the next step, transitions are integrated at both ends of the designed FSIW. The central septum is tapered to a 50 Ω impedance microstrip width over a length of L_t with part of the upper ground plane precisely above it removed in a triangular shape for field matching. In addition, the upper substrate with an upper ground plane dimension of $L_m \times W_m$ is cut and removed to constitute microstrip segments at both ends. The SFSIW, with the integrated transition at both ends, is shown in Fig. 2.

Fig. 3 shows the S-parameter response for the designed half wavelength FSIW segment with transitions at two ends. The designed FSIW covers almost the entire Ku-band with a bandwidth of 9 GHz (12.7–21.7 GHz) and minimum insertion loss of 0.73 dB. Current distribution on the central septum and electric field variation over the designed FSIW

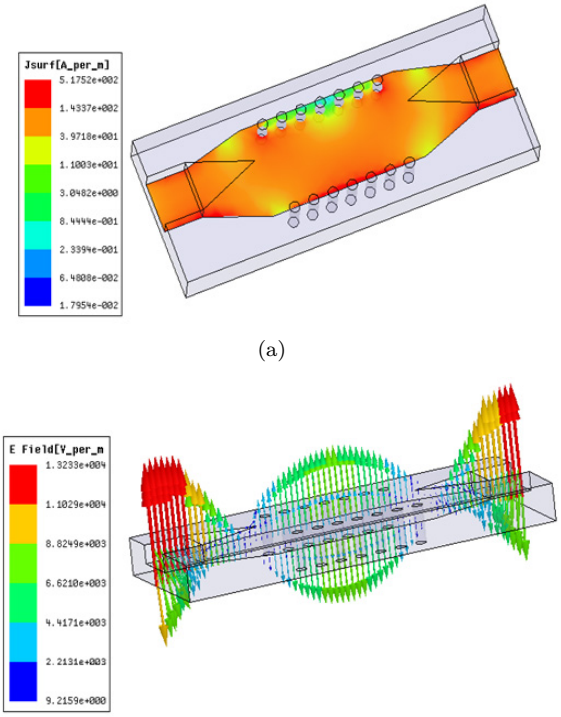

Fig. 4: *(a) Current distribution in central metal septum of FSIW with transitions and (b) electric field transition between FSIW and microstrip.*

with transitions at 14 GHz are shown in Figs. 4(a) and 4(b), respectively. The current distribution is almost uniform and the field between the FSIW and microstrip line exhibits smooth transformation.

2.3 Cutting a Slot on the Central Metal Septum of the Half Guided Wavelength FSIW

In this section, the SFSIW segment is designed and the effects on the position (distance between one of the edges of the central septum and center of the slot), width, and length of the slot are analyzed.

2.3.1 Variation in the slot position

A slot 0.5 mm in width and 3 mm in length is inserted onto the central metal septum of the FSIW segment as shown in Fig. 2. The position 'P' of the slot varies according to the different values, keeping breadth 'b' and length 'a' constant. For clarity, S-parameter responses for only three slot positions are shown in Fig. 5 where $P = 1.175$ mm, $P = 2.175$ mm (center), and $P = 3.175$ mm. As the slot position moves away from the septum edge (shown in Fig. 2), the cut off frequency shifts toward the higher end of the frequency spectrum, thus reducing the bandwidth. A maximum shift of 7.2% is observed, which is negligible.

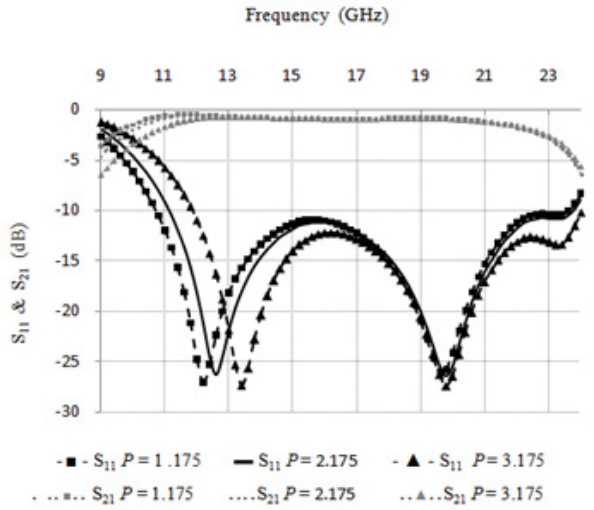

Fig. 5: *S-parameter response of the SFSIW structure with varying values of slot position 'P' (in mm).*

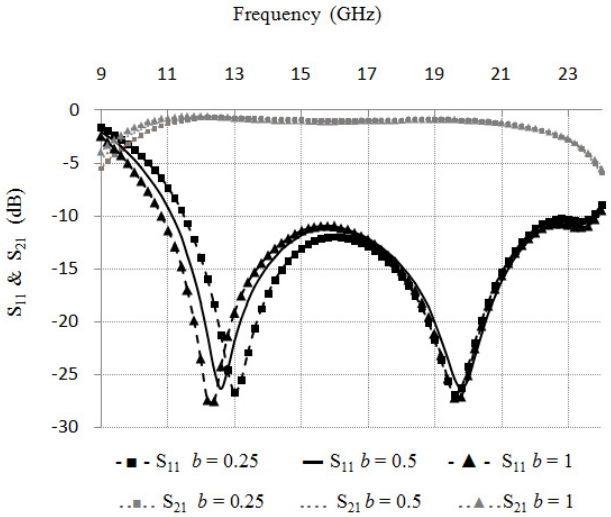

Fig. 6: *S-parameter response of the SFSIW structure with varying values of slot width 'b' (in mm).*

2.3.2 Variation in slot width

In the next step, the slot width is varied from 0.25 to 1.0 mm, keeping the position and length fixed at $P = 2.175$ mm (center) and $a = 3$ mm, respectively. Fig. 6 shows the S-parameter response for width values $b = 0.25$, 0.5, and 1 mm. With an increase in the slot width, the cut off frequency shifts toward the lower end of the frequency spectrum, thereby increasing the bandwidth. However, the maximum shift is only 3.6% which is insignificant.

2.3.3 Variation in slot length

Next, the length of the centrally placed slot on the central septum is varied, keeping the position and width constant at $P = 2.175$ mm (center) and $b =$

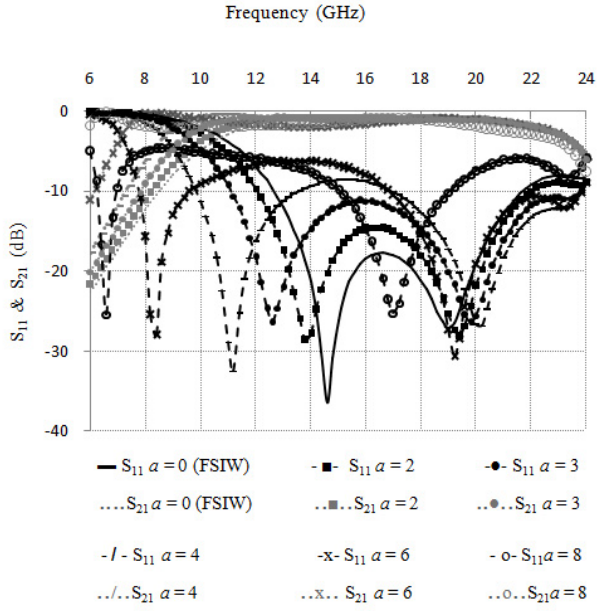

Fig. 7: *S-parameter response of the SFSIW structure with varying values of slot length 'a' (in mm).*

0.5 mm, respectively. Length 'a' is varied through $a =$ 0 mm (no slot) to $a = 8$ mm (maximum length of the FSIW). Fig. 7 shows the S-parameters of the SFSIW segment with different slot lengths. A shift in cut off frequency toward the lower end of the frequency spectrum is observed with an increase in slot length. In this case, the cut off frequency shifts by 50.39%, from $f_c = 12.7$ GHz for $a = 0$ mm to $f_c = 6.3$ GHz for $a = 8$ mm. It is also evident from the graph that for lower slot lengths $a = 0$ to 3 mm the structure shows a single band, whereas for higher slot lengths the band is bifurcated into two, due to the reactive impedance of the inserted slot.

It can be inferred from the study that the variation in slot length has a significant effect on the performance of the SFSIW structure, whereas the position and width can be used for fine-tuning if required. The increase in length response is therefore further investigated using the lumped equivalent circuit and electric field analysis.

2.4 Detailed Analysis of Length Variation in a Centrally Placed Slot

The following sections present a detailed analysis concerning the effects of length variation on a centrally placed slot. The HFSS and ADS simulation software are used for the electric field and lumped equivalent circuit analysis, respectively.

2.4.1 Deriving a lumped equivalent circuit

Initially an approximate lumped equivalent of the SFSIW structure is derived, as shown in Fig. 8.

For the metal plates, two plate transmission line

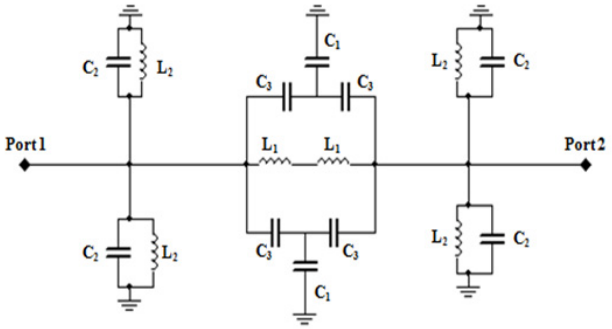

Fig. 8: *Approximate equivalent circuit of the proposed SFSIW structure.*

modeling is used, and via wires modeled as inductors [17, 23], whereas ohmic losses are neglected. Plate inductors are referred to as L_1 with L_2 representing via wire inductors. Capacitors C_1 represent the capacitance between the central metal septum and two grounds in the central part of the FSIW segment along with fringing capacitance due to slot edges. Capacitors C_2 represent capacitance between the central septum and two ground planes at the ends of the FSIW segment along with fringing capacitances at plate edges. Capacitors C_3 represent the capacitance between via wires and metal plates. Circuit component values for the FSIW segment consist of $L_1 = 0.7$ nH, $L_2 = 0.351$ nH, $C_1 = 0.005$ pF, $C_2 = 0.175$ pF, and $C_3 = 0.32$ pF.

Introduction of the slot provides additional capacitance and inductance into the circuit. Babinet's principle is used to find the reactance value [24]. Slot capacitance comes in parallel with C_3 capacitors, increasing its overall value. For lower slot lengths, capacitance between the two metal plates is dominant, decreasing the overall value of C_1 due to the removal of the metal from the central part of the SFSIW septum. Whereas for higher slot lengths fringing capacitance plays a dominant role resulting in an overall incremented value for capacitor C_1. Capacitors C_2 which include the central septum to ground capacitances at both ends of SFSIW and fringing capacitance at the edges are not affected by slot loading. The effect of inductance is negligible for these slot lengths. Fig. 9 shows the response of equivalent circuits in the structure with increasing slot length.

Using HFSS and ADS, two frequencies f_{01} and f_{02} at which return losses are minimum for various slot lengths are compared in Table 1, and the C_1 and C_3 values presented.

The lower peak shifts toward the lower end of the frequency spectrum with an increase in the slot length due to the rising value of C_3, thereby explaining the slow-wave effect. Whereas a decrease in the C_1 value for the lower slot lengths shifts the higher peak

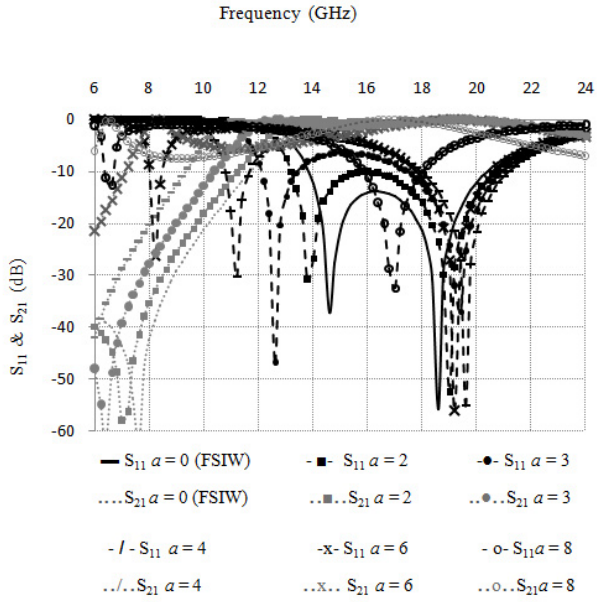

Fig. 9: *S-parameter response of the equivalent SFSIW circuit structures with varying slot length values 'a' (in mm).*

Table 1: *Comparison of two peak frequencies of SFSIWs with varying slot lengths, simulated in HFSS and ADS.*

	HFSS		ADS			
a (mm)	f_{01} (GHz)	f_{02} (GHz)	f_{01} (GHz)	f_{02} (GHz)	C_1 (pF)	C_3 (pF)
0	14.6	19	14.6	18.8	0.005	0.32
2	14	19.4	13.8	19	0.003	0.37
3	12.6	19.8	12.6	19.4	0.002	0.45
4	11.2	20.2	11.2	19.6	0.001	0.6
6	8.2	19.2	8.2	19.2	0.003	1.2
8	6.6	17	6.6	17	0.15	2

toward the higher end of the frequency spectrum while an increase in C_1 for the higher slot lengths shifts the higher pass band toward the lower end of the frequency band. The variations in circuit components with slot lengths deteriorate the S_{11} response in the middle of the frequency spectrum, causing a filtering effect. All the effects mentioned result in a decrease in the cut off frequency and an overall increase in the bandwidth with a rise in the slot length until it reaches 3 mm. For higher slot lengths, the structure acts as a dual band structure.

2.4.2 Propagating modes in SFSIWs

To study mode propagation, the following electric field patterns are observed: 15 GHz for the FSIW segment, 12.6 GHz for the SFSIW where $a = 3$ mm, 19.8 GHz for the SFSIW where $a = 3$ mm, 6.6 GHz for the SFSIW where $a = 8$ mm, and 17 GHz for the SFSIW where $a = 8$ mm, as shown in Figs. 10–14, respectively. The TE_{10} mode propagates in a complete passband of FSIW and SFSIW with a slot length of 3 mm. Figs. 10–12 show similar patterns. Whereas in the SFSIWs with slot lengths of 8 mm the two passbands have two different modes; TE_{10} and TE_{20}. Mode TE_{10} propagates in the lower passband as shown in Fig. 13, while TE_{20} propagates in the upper passband as shown in Fig. 14.

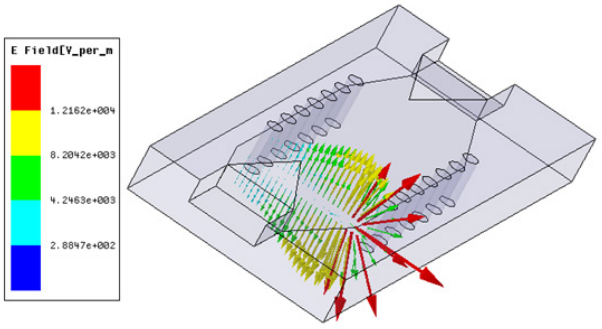

Fig. 10: *Electric field pattern of TE_{10} mode propagating in FSIW segment at 15 GHz.*

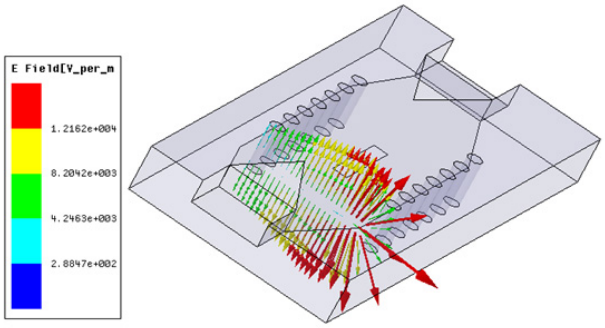

Fig. 11: *Electric field pattern of TE_{10} mode propagating in SFSIW where $a = 3$ mm at 12.6 GHz.*

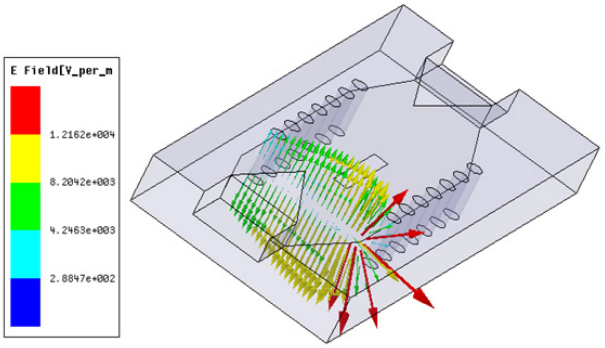

Fig. 12: *Electric field pattern of TE_{10} mode propagating in SFSIW where $a = 3$ mm at 19.8 GHz.*

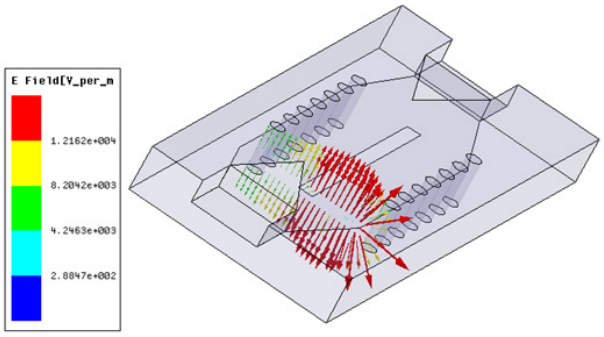

Fig. 13: *Electric field pattern of TE_{10} mode propagating in SFSIW where $a = 8$ mm at 6.6 GHz.*

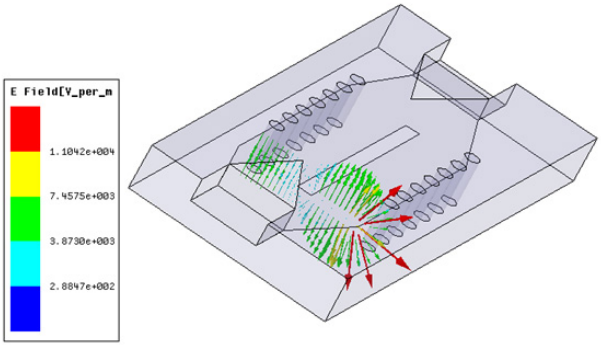

Fig. 14: *Electric field pattern of TE_{20} mode propagating in SFSIW where $a = 8$ mm at 17 GHz.*

3. RESULTS AND DISCUSSION

The FSIW segment and the SFSIW with a centrally placed slot, where $a = 3$ mm and $b = 0.5$ mm, are fabricated and their S_{11} and S_{21} parameters measured to validate the simulated results. Photographs showing different layers of the structure during the fabrication process for the SFSIW are presented in Fig. 15. The measured results are compared with the simulated S-parameter responses obtained from HFSS and ADS for FSIW and SFSIW in Figs. 16 and 17, respectively. Responses are shown until 20 GHz is reached, as indicated by the available VNA measurement.

The measured and simulated results are in good agreement using both HFSS and ADS, except at higher frequencies. The discrepancies in the measured results are mainly due to fabrication and alignment errors. Even a small deviation during fabrication can result in significant errors at higher frequencies.

The FSIW and all SFSIWs cover useful frequencies for space communication. The SFSIW with slot dimensions where $a = 3$ mm and $b = 0.5$ mm provide the best wideband response and the SFSIW where $a = 8$ mm and $b = 0.5$ mm exhibit the most compact filter when compared with different microstrip lines and SIW-based filters.

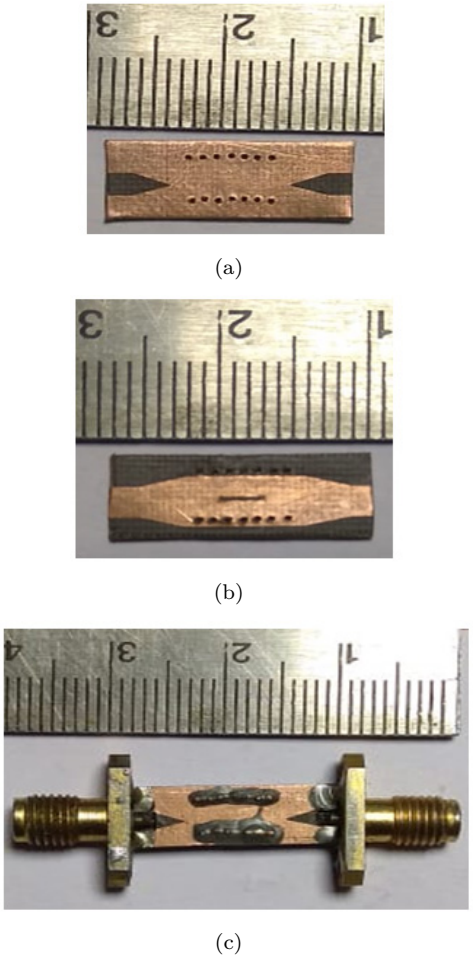

(a)

(b)

(c)

Fig. 15: *Photographs showing SFSIW fabrication, (a) upper substrate layer with top ground plane, (b) lower substrate layer with a slot ($a = 3$ mm, $b = 0.5$ mm) on the central metal septum, and (c) fabricated SFSIW with transitions and SMA connectors.*

Table 2: *Comparison of SFSIW where $a = 3$ mm with different reported wideband structures.*

Ref.	Structure	Center Frequency (GHz)	S_{21} (dB)	Size λ_g^2	Bandwidth (%)
[13]	SIW	6.88	<2	1.69	40
[15]	SIW	14.84	<2.06	4.3	41.5
[17]	SIW	8.98	<1.5	1.18	47.4
[6]	Microstrip	4.3	<0.9	0.61	37.2
SFSIW ($a = 3$ mm)	SIW	16.6	<2	0.94	67.5

It is evident from Table 2 that the slot loaded FSIW where $a = 3$ mm, exhibits the highest bandwidth, whereas Table 3 shows that the slot loaded FSIW where $a = 8$ mm provides the smallest size and lowest insertion loss. Moreover, the structures are very simple to implement.

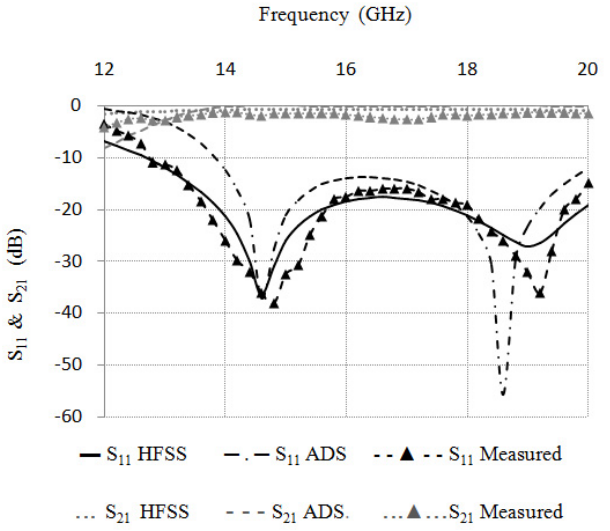

Fig. 16: *S_{11} and S_{21} responses of the FSIW segment with transitions.*

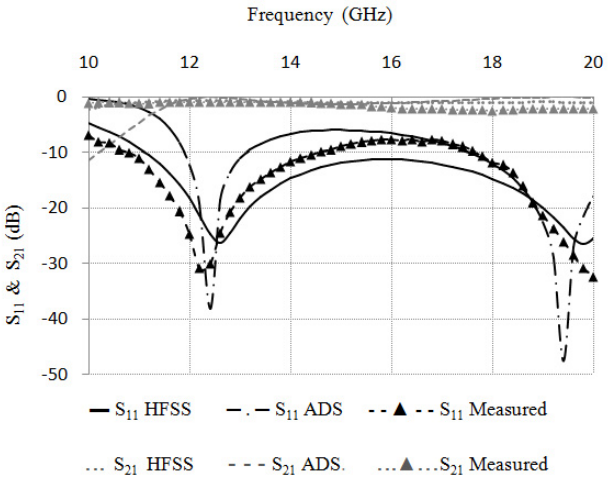

Fig. 17: *S_{11} and S_{21} responses of the SFSIW ($a = 3\,mm$, $b = 0.5\,mm$) with transitions.*

4. CONCLUSION

Slot loading in a central metal septum of the FSIW segment exhibits two phenomena: slow wave and filtering, which are explained in detail with the help of equivalent circuits and field diagrams in this paper. Both phenomena have been exploited for various structures applicable to space communication by using the appropriate slot size and position. The discussed phenomena can be used to develop various structures such as filters and antennas for different frequency bands.

Table 3: *Comparison of SFSIW where $a = 8\,mm$ with different reported compact filters.*

Ref.	Structure	Center Frequency (GHz)	S_{21}[¶] (dB)	Size λ_g^2	Bandwidth (%)
[16]	SIW	5.75	2.05	0.533	3.66
[14]	SIW	5	1.3	0.577	5
[7]	Microstrip	5.4	0.5	0.427	10
[18]	SIW	11.185	0.82	0.204	4.12
SFSIW ($a = 8\,mm$)	SIW	6.65	0.2	0.151	10.52

[¶]at center frequency

REFERENCES

[1] K. Wu, D. Deslandes, and Y. Cassivi, "The substrate integrated circuits – A new concept for high frequency electronics & optoelectronics," in *6th International Conference on Telecommunications in Modern Satellite, Cable and Broadcasting Service (TELSIKS 2003)*, 2003, pp. P-III–P-X.

[2] K. Wu, "Towards the development of terahertz substrate integrated circuit technology," in *2010 Topical Meeting on Silicon Monolithic Integrated Circuits in RF Systems (SiRF)*, 2010, pp. 116–119.

[3] M. Bozzi, L. Perregrini, K. Wu, and P. Arcioni, "Current and future research trends in substrate integrated waveguide technology," *Radioengineering*, vol. 18, no. 2, pp. 201–209, June 2009.

[4] M. Bozzi, A. Georgiadis, and K. Wu, "Review of substrate integrated waveguide circuits and antennas," *IET Microwaves, Antennas and Propagation*, vol. 5, no. 8, pp. 909–920, June 2011.

[5] W. Che, L. Geng, K. Deng, and Y. L. Chow, "Analysis and experiments of compact folded substrate-integrated waveguide," *IEEE Transactions on Microwave Theory and Techniques*, vol. 56, no. 1, pp. 88–93, Jan. 2008.

[6] S. Moitra, R. Dey, and P. S. Bhowmik, "Design and band coalition of dual band microstrip filter using DGS, coupled line structures and series inductive metallic vias," *Analog Integrated Circuits and Signal Processing*, vol. 101, pp. 77–88, 2019.

[7] A. Kumar and M. V. Kartikeyan, "A design of microstrip bandpass filter with narrow bandwidth using DGS/DMS for WLAN," in *2013 National Conference on Communications (NCC)*, New Delhi, India, 2013.

[8] F. Chen, N. Zhang, P. Zhang, and Q. Chu, "Design of ultra-wideband bandstop filter using defected ground structure," *Electronics Letters*, vol. 49, no. 16, pp. 1010–1011, 1 Aug. 2013.

[9] K. H. Chiang and K. W. Tam, "Microstrip monopole antenna with enhanced bandwidth using defected ground structure," *IEEE Antennas and Wireless Propagation Letters*, vol. 7, pp. 532–535, 2008.

[10] M. Akbari, S. Zarbakhsh, and M. Marbouti, "A novel UWB antenna with dual-stopband char-

acteristics," *Microwave and Optical Technology Letters*, vol. 55, no. 11, pp. 2741–2745, Nov. 2013.

[11] Y. J. Sung, C. S. Ahn, and Y. Kim, "Size reduction and harmonic suppression of rat-race hybrid coupler using defected ground structure," *IEEE Microwave and Wireless Components Letters*, vol. 14, no. 1, pp. 7–9, Jan. 2004.

[12] M. Naghshvarian-Jahromi and M. Tayarani, "Defected ground structure band-stop filter by semi-complementary split ring resonators," *IET Microwaves, Antennas & Propagation*, vol. 5, no. 11, pp. 1386–1391, 19 August 2011.

[13] J. Jin and D. Yu, "Substrate integrated waveguide band-pass filter with coupled complementary split ring resonators," in *2014 XXXIth URSI General Assembly and Scientific Symposium (URSI GASS)*, Beijing, China, 2014, pp. 1–4.

[14] L. Wu, X. Zhou, Q. Wei, and W. Yin, "An Extended Doublet Substrate Integrated Waveguide (SIW) Bandpass Filter With a Complementary Split Ring Resonator (CSRR)," *IEEE Microwave and Wireless Components Letters*, vol. 19, no. 12, pp. 777–779, Dec. 2009.

[15] F. T. Liang and X. An, "Wideband bandpass filters using corrugated substrate integrated waveguide and periodic structures" *Microwave and Optical Technology Letters*, vol. 57, pp. 2665–2668, 2015.

[16] Y. L. Zhang, W. Hong, K. Wu, J. X. Chen, and H. J. Tang, "Novel substrate integrated waveguide cavity filter with defected ground structure," *IEEE Transactions on Microwave Theory and Techniques*, vol. 53, no. 4, pp. 1280–1287, April 2005.

[17] C. Liu, and X. An, "A SIW-DGS wideband bandpass filter with a sharp roll-off at upper stopband," *Microwave and Optical Technology Letters*, vol. 59, no. 4, pp. 789–792, Apr. 2017.

[18] N. Muchhal and S. Srivastava, "Design of miniaturized high selectivity folded substrate integrated waveguide band pass filter with Koch fractal," *Electromagnetics*, vol. 39, no. 8, pp. 571–581, 2019.

[19] J. Y. Sze and K. L. Wong, "Slotted rectangular microstrip antenna for bandwidth enhancement," *IEEE Transactions on Antennas and Propagation*, vol. 48, no. 8, pp. 1149–1152, Aug. 2000.

[20] D. Jia, J. Deng, Y. Zhao, and K. Wu, "Multilayer SIW dual-band filters with independent band characteristics and high selectivity," *Frequenz*, vol. 73, no. 9–10, pp. 293–300, 2019.

[21] "Radio Frequencies for Space Communication". Australian Space Academy. `https://www.spaceacademy.net.au/spacelink/radiospace.htm`

[22] S. Kumari, V. R. Gupta, and S. Srivastava, "Analysis of staggered-via loss in substrate integrated waveguide," *IETE Journal of Research*, 2020.

[23] D. M. Pozar, *Microwave Engineering*, 3rd ed. India: Wiley, 2009.

[24] C. A. Balanis, *Antenna Theory Analysis and Design*, 2nd ed. India: Wiley, 2009.

Sheelu Kumari received her B.E. (Electronics and Communication Engineering) in 2002 from Gulbarga University, Karnataka, India. She received Master's degree in Electronics and Communication Engineering from Birla Institute of Technology, Mesra, Ranchi, India in 2012. Presently she is pursuing Ph.D. from Birla Institute of Technology, Mesra, Ranchi, India. She has several publications in international and national journals. She has presented many papers in several international and national conferences. Her areas of interest include millimeter-wave and microwave propagation, substrate integrated circuits, etc.

Vibha Rani Gupta received her Bachelor's, Master's and Ph.D. degrees in Electronics and Communication Engineering all from Birla Institute of Technology, Mesra Ranchi, India in 1986, 1994, and 2007, respectively. She joined Birla Institute of Technology as a faculty in the year 2002. Presently she is Professor at the department of Electronics and Communication Engineering, BIT, Mesra, Ranchi. She has authored and coauthored more than 74 technical journal articles and conference papers. Her research interests are Antennas and MICs for Wireless Communication and Microwave measurement of materials. She is members of several professional bodies such as IEEE, ISTE, IAENG, ICEIT and Fellow of IETE and IE.

Shweta Srivastava received her B.Tech degree from Institute of Peoples Science and Technology, Chitrakoot, India in 1998 and Ph.D. degree from Indian Institute of Technology, Banaras Hindu University, Varanasi, India in 2002. She joined Birla Institute of Technology, Mesra, Ranchi, India in February 2002 as a faculty member. She was awarded SERC fast track project for young Scientist by Department of Science and Technology, Government of India. She joined Jaypee Institute of Information Technology, Noida, India in 2014 and is presently serving there as Professor and Head of the Department of Electronics and Communication Engineering. She has published more than 80 research papers in peer reviewed and reputed journals and conferences. She was awarded Smt. Ranjana Pal Memorial Award from IETE and the award for outstanding women in engineering by Venus foundation. Her areas of interest include microwave circuits and antennas, microstrip technology, substrate integrated waveguides, millimeter wave technology, etc.